

TARGET CLASSIFICATION NEAR COMPLEX INTERFACES USING TIME-FREQUENCY FILTERS

Nicole Gache, Patrick Chevret and Véronique Zimpfer

CPE Lyon, LISA/LASSSO (EP00092 CNRS)
43, Bd du 11 novembre 1918 - BP 2077 - 69616 Villeurbanne cedex - France
e-mail : gache@cpe.fr

ABSTRACT

This paper presents a method for target recognition and classification in shallow water environment. It is based on time-frequency filtering matched to a free field reference target response. The decision strategy lies on the comparison of the reference and the filter output signal. The method is applied to an experimental data base containing target acoustic responses measured in a tank for typical configurations (free field, semi-infinite space and waveguide). First, the recognition of a spherical shell is carried out. The obtained rate of recognition and confusion are more than encouraging. Then, a classification procedure is conducted and a degradation of the mean performances is to be noted in the more general case. However, the classification of 3D targets independently of their attitude gives quite satisfactory results.

1. INTRODUCTION

The target scattering inverse problem in an opaque environment is a recurrent theme in underwater acoustics. Common applications are imaging of buried objects in sediments, detection and localization, recognition and classification of targets in oceanic waveguides.

As concerns detection and localization problems, the traditional inversion techniques lie on matched field processing that needs *a priori* informations on the propagation medium [12, 13, 10].

In the case of target recognition or classification, the difficulty is to identify on the target response relevant parameters that best summarize its geometrical and mechanical properties. Previous studies have shown that a wide band approach based on time-frequency (TF) description suits particularly well for this task and for the understanding of echo formation mechanisms [9, 4]. The efficiency of Wigner-Ville distribution (WVD) based methods was shown in the case of (1) shells/solid targets classification from tank measurements [8] and (2) classification of spherical and cylindrical targets (according to their mechanical properties) from their numerical responses [2].

In a multipath environment, some expected degradations of the performances were demonstrated in the case of numerical target

responses for simple waveguides [1]. These degradations should be pronounced in real underwater conditions where many factors modify the signal transient (rough surface boundaries, refraction index variations and many kind of noise) and contribute to a loss of resolution between successive echo wave packets.

The inversion method we present in this paper (that could be extended to detection and localization problems) does not need an *a priori* knowledge of the medium like for matched field processing methods. On the contrary, it consists of a TF filter matched to a reference (known) free field target (or kind of targets) response. The recognition or classification process is performed thanks to a minimization of the quadratic error between the filter output signal and the reference signal.

2. TIME-FREQUENCY PROJECTION FILTERING

As TF distributions are very useful tools for the observation and the understanding of echo formation, a TF filtering method seems to be the more pertinent approach for the extraction of target echoes from altered signals.

The Wigner-Ville distribution (WVD) [3, 5] associated to the broadband response of a free field spherical target is presented on figure 1 as well as the impulse response and the associated pressure density spectrum. The different patterns that appear on this picture can be identified and classified in two categories [9, 11]:

- interferences due to the bilinear nature of the WVD. They do not correspond to any physical propagation phenomena.
- very energetic patterns. The first one is associated to the specular echo and the two next correspond to surface waves arrivals (antisymmetric Lamb waves a_0^- and a_0^+).

The TF filter to be derived must take in account these physical considerations. Thus, it will be based on a region of the TF plane that contains the echoes identified as pertinent, *e.g.* the specular and the surface waves echoes. Such an approach has been developed by F. Hlawatsch *et al.* and called time-frequency projection filtering [7]. This region, called R , defines the TF support of the time-varying filter : every component outside the region R on the signal to be filtered will be rejected. An indicator function $I_R(t, f)$ is associated to R and equals 1 if $(t, f) \in R$ and 0 outside.

The time-varying filter to design has an impulse response $h(t, t')$. When excited by a finite-energy signal $x(t)$, its output signal can be written as

$$y(t) = \int_{t'} h(t, t') \cdot x(t') dt'.$$

This work was supported by the french ministry of defense DGA (GESMA)

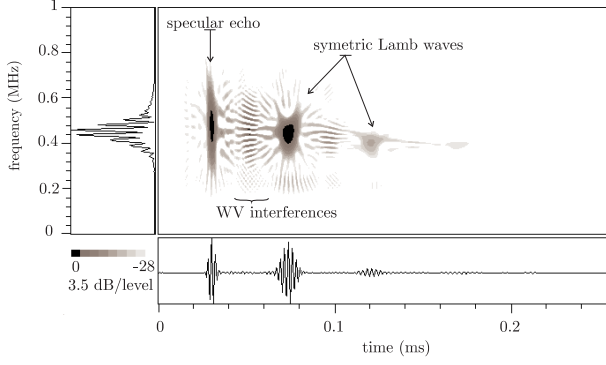


Figure 1: Wigner-Ville distribution of the experimental response of an aluminium spherical shell (target 1).

$y(t)$ is an element of a linear signal space \mathcal{S} , subspace of the finite-energy signals space $\mathcal{L}_2(\mathbb{R})$. $h(t, t')$ can be interpreted as the kernel of an orthogonal projection operator of \mathcal{S} . The optimal signal space is the one whose WV distribution W_S [6] is the closest to the indicator function $I_R(t, f)$ according to two criteria [7].

The first one concerns maximization of the concentration of \mathcal{S} on R . Since the WVD of a signal describes the signal's energy distribution in the TF plane, W_S describes the \mathcal{S} 's TF energy distribution. The concentration of \mathcal{S} on the region R is defined as the ratio of the space's energy in R and the total energy.

The second one deals with minimization of a localization error $\varepsilon(\mathcal{S}, R)$ between \mathcal{S} and the region R . It characterizes the deviation of W_S from the idealized function I_R filling out R energetically.

The indicator function of a region R is not a valid WVD of a space but it can always be written as an infinite linear combination of WVD of orthonormal signals $u_k(t)$ [7] :

$$I_R(t, f) = \sum_{k=1}^{\infty} \lambda_k W_{u_k}(t, f).$$

u_k and λ_k are respectively the eigensignals and real-valued eigenvalues of the eigenequation

$$\int_{t'} h_R(t, t') \cdot u_k(t') dt' = \lambda_k u_k(t)$$

where the Hermitian kernel h_R is directly obtained from the region R and its indicator function

$$h_R(t, t') = \int_{-\infty}^{+\infty} I_R\left(\frac{t+t'}{2}, f\right) \exp(2i\pi(t-t')f) df.$$

As the previous eigensignals u_k define an orthonormal basis spanning a space of infinite dimension, a reduced set of $u_{k(k=1, \dots, N)}$ defines a N -dimensional eigensubspace $\mathcal{U}_R^{(N)}$ of this space. It can be shown [7] that the signal space \mathcal{S} for which the concentration $\rho(\mathcal{S}, R)$ is maximum corresponds to the eigenspace $\mathcal{U}_R^{(N)}$ spanned by the N dominant eigensignals $u_k(t)$ associated to the N largest eigenvalues λ_k . Then, the squared localization error $\varepsilon^2(\mathcal{S}, R)$ is minimum when N corresponds to the number of eigenvalues greater than $1/2$.

Once \mathcal{S} identified to $\mathcal{U}_R^{(N)}$, the orthogonal projection operator h , can be expressed in terms of the orthonormal basis $\{u_k\}$:

$$h(t, t') = \sum_{k=1}^N u_k(t) \times u_k^*(t')$$

As an example, if the reference signal used to elaborate the operator h is the spherical aluminium shell response of figure 1, the optimal dimension of the subspace is 5 and the localization error and the concentration are respectively 1 % and 90 %.

3. THE EXPERIMENTS

The measurements were conducted in a tank of 2 m length, 1 m wide and 1 m high. Six different targets were selected (*cf.* table 1) and three series of experiments were led :

- in free field (one signal by target, namely 6 signals),
- in semi-infinite field in order to include reflection and reverberation by different interfaces,
- in 3 different waveguide configurations to include multiple reflections (only for the spherical shell).

target 1	spherical shell in aluminium of diameter 30 mm and thickness 0.6 mm
target 2	cylindrical shell in aluminium of diameter 40 mm and thickness 2 mm. Its length is large compared to the transducer beam. The inner fluid is air.
target 3	same as target 2, except for the inner fluid that is water.
target 4	aluminium cylindrical solid target with hemispherical endcaps. The diameter is 30 mm, the length is 75 mm. The major axe is lined up with the transducer beam.
target 5	same as target 4, except for the attitude in the transducer beam : the major axe is perpendicular to the transducer beam.
target 6	spherical solid target of marble of diameter 30 mm.

Table 1: Targets description

As concerns the semi-infinite propagation, the targets were located at the vicinity of 4 different interfaces : a non reverberating one (free surface), a layer of thin sand, a slab of marble and a sheet of gravel. For each configuration, the target response was recorded for 4 immersions : in contact with the interface and 1 cm to 3 cm far from it. This series of measurements gives a set of 100 acoustic target responses.

For the shallow water waveguide situations, the small length of the tank does not permit to modelize long range propagation but the transceiver-target separation is large enough (1.2 m) to include multiple reflections on the free surface and the sediment bottom. In the whole series, both the target (spherical aluminium shell) and the transceiver are located at the middle of the watercolumn. In the first situation, the height of the watercolumn is 30 cm (10 target diameter), the bottom is made up of sand. In the second one, the water height is decreased to 15 cm. For the last one a sheet

made up of gravel is put on the sand bottom at a middle distance between the transmitter and the target.

For any measurements, the transmitted signal, issued from a broadband transducer, is a pulse of about $6 \mu\text{s}$ duration with a frequency band centered on 500 kHz. The beamwidth at 500 kHz is 6° (-3 dB). The whole data base is finally composed of 109 signals whose general structure is very different from each other and complex in all cases.

4. TARGET RECOGNITION

4.1. The recognition procedure

The recognition procedure requires different stages. First, the free field response $r(t)$ of the reference target to be recognized is used to design the TF projection filter according to the method described in section 2. In order to identify the specular echo of any signal $x(t)$ to be analyzed, the filter has to be applied as a sliding window along the signal $x(t)$. For each location t_0 of the filter on the signal, a quadratic error $\mathcal{E}^2(t_0)$ between the normalized envelopes of $r(t)$ and the output signal $y(t, t_0)$ is calculated. The date t_{opt} corresponding to the minimum of $\mathcal{E}^2(t_0)$ can be identified with the date of apparition of the specular echo. The associated output signal $y(t, t_{\text{opt}})$ is taken as the result of the filtering procedure.

As an example, figure 2(a) presents the response of the aluminium spherical shell located 2 cm above the bottom of gravel while figure 2(b) shows the output signal of the filter designed from the free field response of the same target. The arrow on the curve (a) gives the date t_{opt} of the specular echo.

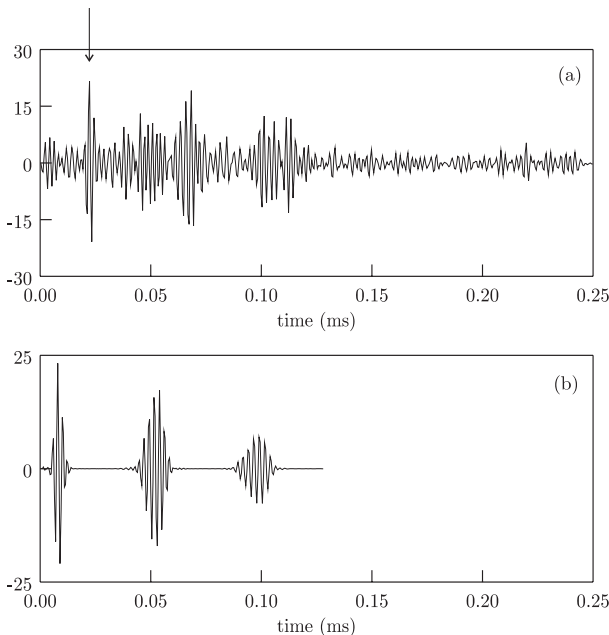


Figure 2: Example of TF projection filtering. The filter is designed from the free field spherical shell response. (a) Experimental response of the same target located 2 cm above the sheet of gravel. (b) Filter output signal.

In order to avoid confusion between low reverberation signals and target echoes, we consider the ratio \mathcal{A} between maximum am-

plitudes of the input $x(t)$ and the output $y(t, t_{\text{opt}})$. A low value of \mathcal{A} , limited by a threshold η_A , must lead to reject the reference target occurrence hypothesis. If this first test leaves a possibility of the reference target presence, it remains to compare $\mathcal{E}^2(t_{\text{opt}})$ to a threshold $\eta_\mathcal{E}$ whose value depends on the target to recognize.

4.2. The spherical shell recognition

The reference signal $r(t)$ is the free-field response of the spherical shell (target 1). The recognition procedure described in section 2 is applied to the 100 signals obtained in semi-infinite space. The filtering operation is applied to each signal and the quadratic error $\mathcal{E}^2(t_{\text{opt}})$ is calculated.

Whatever the signal coming from the spherical shell (target 1), $\mathcal{E}^2(t_{\text{opt}})$ is always smaller than 6.5 % of the reference signal energy. This threshold value $\eta_\mathcal{E} = 6.5 \%$ and an amplitude threshold η_A of 0.4 entails 100 % of recognition rate and 5 % of confusion rate.

Detailed recognition results can be expressed for the four different interfaces : partial confusion rates are given in table 2. These results are very encouraging for two main reasons. First, the confusion rates are small for any configurations. Then, attenuating sand bottom, which is statistically the more common at the vicinity of the coasts (shallow water), allows a complete recognition of the spherical shell. The worst confusion rates are obtained for the perfectly rigid surface, that will not be (statistically) encountered in an ocean environment.

interface	sand	marble	gravel	free surface
confusion rate	0 %	10 %	5 %	5 %

Table 2: Confusion rates for spherical shell recognition depending on interface nature ($\eta_\mathcal{E} = 6.5 \%$ and $\eta_A = 0.4$)

As concerns the recognition rates in free field and in the three waveguides, the suggested method is very high-performance : the recognition rate is 100 % and the confusion one is 0 %. Nevertheless, these results are not definitive for the waveguide configurations. Indeed, the transducer beam is too narrow to produce an effectiveinsonification of the free surface and the bottom. Only a small part of the energy is reflected back to the receiver.

5. TARGET CLASSIFICATION

In this section, the recognition method is extended to a classification procedure that consists of classifying the whole data base in the categories represented by the 6 target configurations described in table 1.

In the first step, the six filters associated to the six targets in the free field are synthesized. Secondly, the set of signals are projected on each filter. Then, the belonging class of a signal \mathcal{C} is determined by the minimum projection error on the set of filters.

$$\mathcal{C} = \underset{i=1,\dots,6}{\arg \min} \{ \mathcal{E}_i^2(t_{\text{opt}}) \}$$

The classification results are presented on figure 3 in the form of a confusion matrix (confrontation between the real and the estimated classes). Each element includes all the surfaces and target immersions. The results are not as good as expected and give

the limitations of our recognition method: the identification is not possible for all the targets and, in particular, no identification is possible between targets with different attitude in the transducer beam or with different inner fluids.

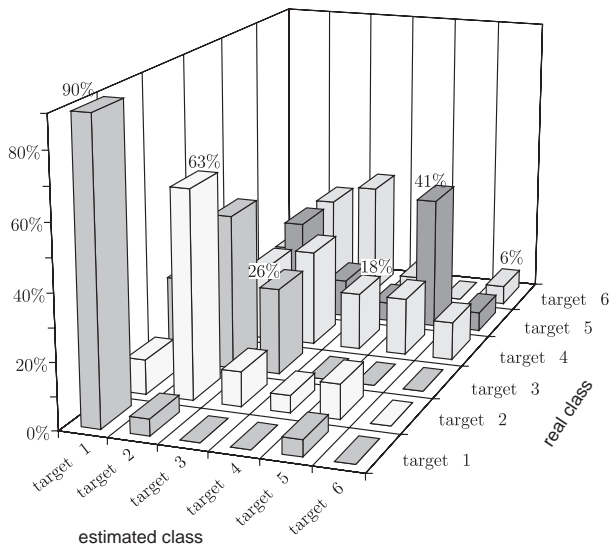


Figure 3: Classification of the whole data base ($\eta_A = 0.4$)

Discarding the two cylindrical shells (targets 2 and 3) because of the absence of such a 2D geometry in a natural environment like the ocean, the spherical shell recognition rate is 90 % and the cylindrical solid target with hemispherical endcaps one is 85 %. On the other hand, the marble target poses a problem of systematic confusion: only 24 % of successful classification.

These classification examples point out the main difficulties encountered by the method, in particular its inefficiency to recover a perfectly rigid and manufactured target made up of marble. The reassuring news are first, that such perfect natural targets can not be found in nature and, second, that the other targets are generally recovered.

6. CONCLUSION

This study clearly shows the advantages of using a time-frequency filtering based method for the recognition of targets in a complex environment. The procedure applied to the recognition of a spherical aluminium shell among a large variety of signals give 100 % of recognition rate and 5 % of confusion rate.

As concerns classification, the results are strongly dependent on the selected classes. In the case of a 3-dimensional targets classification (between a spherical metal shell, a solid cylinder with hemispherical endcaps and a solid marble sphere), the performances are greatly satisfactory (90 % and 85 % of good classification for the spherical shell and the solid cylinder with endcaps) except for the marble target that was systematically a source of confusion. After a few trials, the method seems to be quite robust to noise added on the reference as well as on the data base, suggesting a good potential for real applications in oceans.

Nevertheless, further investigations need to be led in order to guarantee the feasibility of this approach in real conditions. In

particular, the long range waveguide configuration is to be studied in detail both numerically and experimentally.

7. REFERENCES

- [1] P. Chevret. Man made object classification in shallow water: a hybrid approach. In *3rd Int. Conf. on Theoretical and Computational Acoustics*. to appear, 1997.
- [2] P. Chevret, F. Magand, and L. Besacier. Time-frequency analysis of circumferential wave energy distribution for spherical shells. Application to sonar target recognition. *Applied Signal Processing*, Vol. 3:136–142, 1996.
- [3] L. Cohen. *Time-frequency Analysis*. Signal Processing Series. Prentice Hall, 1995. 299 p.
- [4] L.R. Dragonette, D.M. Druhmheller, C.F. Gaumont, D.H. Hughes, B.T. O'Connor, Nai-Chyan Yen, and T.J. Yoder. The application of two-dimensional signal transformations to the analysis and synthesis of structural excitations observed in acoustical scattering. *Proceedings of the IEEE*, Vol. 84(9):1249–1263, 1996.
- [5] P. Flandrin. *Temps-fréquence*. Hermès, Paris, 1993.
- [6] F. Hlawatsch and W. Kozek. The Wigner distribution of a linear signal space. *IEEE Trans. on Signal Processing*, Vol. 41(3):1248–1258, 1993.
- [7] F. Hlawatsch and W. Kozek. Time-frequency projection filters and time-frequency signal expansions. *IEEE Trans. on Signal Processing*, Vol. 42(12):3321–3334, 1994.
- [8] F. Magand. *Reconnaissance de cibles par sonar actif large bande. Application à des coques de forme simple et à la classification des espèces de poissons en mer*. Thèse de doctorat, Institut National des Sciences Appliquées de Lyon, France, 1996.
- [9] F. Magand and P. Chevret. Time-frequency analysis of energy distribution for circumferential waves on cylindrical elastic shells. *Acta Acustica united with Acustica*, Vol. 82(5):707–716, 1996.
- [10] M. Mazenski and D. Alexandrou. Active, wide band detection and localization in an uncertain multipath environment. *J. Acoust. Soc. Am.*, Vol. 101(4):1961–1970, 1997.
- [11] G.S. Sammelmann, D.H. Trivet, and R.H. Hackman. The acoustic scattering by a submerged, spherical shell. I: The bifurcation of the dispersion curve for the spherical antisymmetric lamb wave. *J. Acoust. Soc. Am.*, 85(1):114–124, 1989.
- [12] Y. Xu and Y. Yan. Boundary integral equation for source localization with a continuous wave sonar. *J. Acoust. Soc. Am.*, Vol. 92(2):995–1002, 1992.
- [13] T.C. Yang and T.W. Yates. Scattering from an object in a stratified medium. I: Frequency dispersion and active localization. *J. Acoust. Soc. Am.*, Vol. 96(2):1003–1019, 1994.